AD-A149 419 COMPARING DIFFERENT THEORETICAL DESIGNS OF SIX-PORT REFLECTOMETER JUNCTIO..(U) ROYAL SIGNALS AND RADAR ESTABLISHMENT MALVERN (ENGLAND) E J GRIFFIN ET AL. 1/1

UNCLASSIFIED APR 84 RSRE-MEMO-3684 DRIC-BR-93573 F/G 9/3 NL

END
FILMED
DTIC

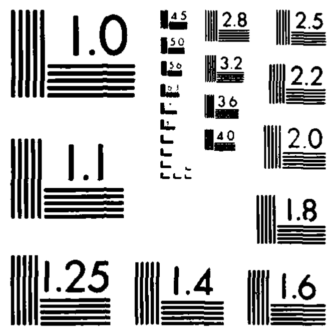

MICROCOPY RESOLUTION TEST CHART
NATIONAL BUREAU OF STANDARDS 1963 A

UNLIMITED

BR93573

(3)

AD-A149 419

RSRE

MEMORANDUM No. 3684

ROYAL SIGNALS & RADAR ESTABLISHMENT

COMPARING DIFFERENT THEORETICAL DESIGNS OF SIX-PORT REFLECTOMETER JUNCTIONS

Authors: E J Griffin and
T E Hodgetts

RSRE MEMORANDUM No. 3684

DTIC FILE COPY

PROCUREMENT EXECUTIVE,
MINISTRY OF DEFENCE,
RSRE MALVERN,
WORCS.

UNLIMITED

84 12 18 139 ~~010~~

ROYAL SIGNALS AND RADAR ESTABLISHMENT

Memorandum 3684

Title: COMPARING DIFFERENT THEORETICAL DESIGNS OF SIX-PORT REFLECTOMETER JUNCTIONS

Authors: E J Griffin and T E Hodgetts

Date: April 1984

SUMMARY

This memorandum presents a derivation of numerical procedures for comparing different theoretical designs of six-port junctions for use in measuring the voltage reflection coefficient Γ of passive loads, ~~$(|\Gamma| \leq 1)$~~. It shows from these that the maximum uncertainty in measuring any passive load can be minimised by a suitable choice of components, in each of four different designs, and discusses the relative merits of these designs in terms of selecting a best compromise for use in a dual six-port network analyser.

Accession For	
NTIS GRA&I	☒
DTIC TAB	☐
Unannounced	☐
Justification	
By	
Distribution/	
Availability Codes	
Dist	Avail and/or Special
A-1	

DTIC COPY INSPECTED 3

RSRE MEMORANDUM NO 3684

COMPARING DIFFERENT THEORETICAL DESIGNS OF SIX-PORT REFLECTOMETER JUNCTIONS

E J Griffin and T E Hodgetts

CONTENTS

1 INTRODUCTION

1.1 Measurement of complex voltage reflection coefficient Γ with a six-port reflectometer was first described by Engen and Hoer (1-3). In this instrument, Figure 1, radiation is directed from a source to the device under test (DUT) by

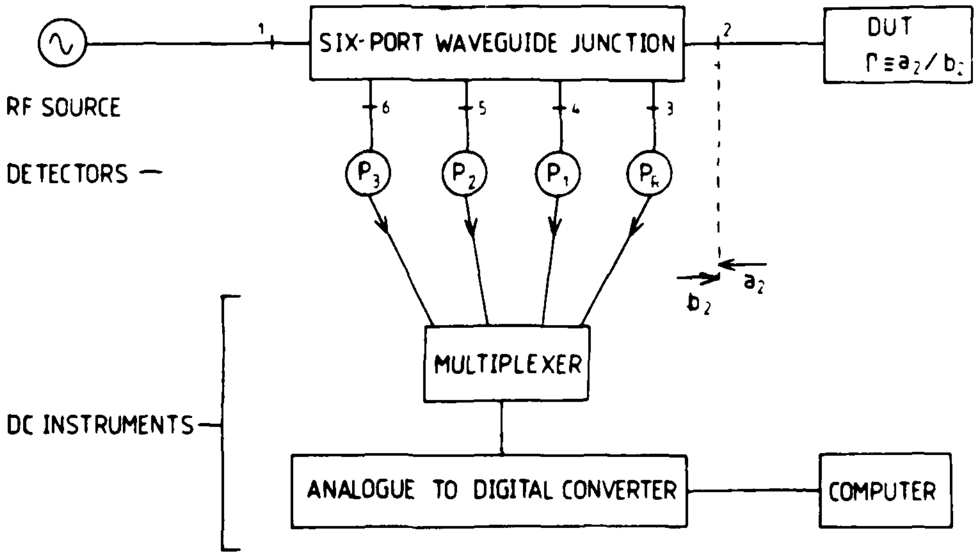

Figure 1 A six-port reflectometer

a six-port waveguide junction which also directs to four square-law detectors different samples of the waves incident on and reflected from the DUT. After calibration (to establish the phase and magnitude relations between these samples in terms of external standards) Γ is calculated from the ratios of outputs $P_K(k=1,2,3)$ from three of these detectors to that from the fourth (reference) detector P_R. A number of different designs of junction have been described for this instrument (4-22) and it has been shown that, given infinite resolution in representing the power ratios in calculation, any constant linear waveguide junction having non-identical transmission between its six ports would suffice (23). Since the detector signal-to-noise ratio is finite in practice, a prospective constructor is faced with the question: "Can the likely performance of these different designs be compared theoretically?" By limiting consideration to the measurement of passive DUTs, so that $|\Gamma|<1$, the tradeoff between uncertainty of measurement and RF power required can be used as a basis for this comparison.

1.2 Specifically, given a maximum level of power P_D permitted at any detector and an equivalent noise power P_N at each detector we derive as criteria for comparing different six-port junction designs:-

(i) the maximum uncertainty U_{max} in measuring any $|\Gamma|<1$ when the reference detector absorbs P_D and

(ii) the maximum power P_{max} that can be incident on the junction without the power at any detector exceeding P_D.

We then show that U_{max} can be minimised for each of four different designs by a suitable choice of components and discuss their relative merits for practical application.

2 MAXIMUM UNCERTAINTY U_{max}

2.1 The power ratios P_k/P_R for a six-port reflectometer such as that of Figure 1 can be related to $\Gamma(\equiv a_2/b_2)$ by an expression of the form:

$$\frac{P_k}{P_R} = \left|\frac{d_k\Gamma+e_k}{c\Gamma+1}\right|^2 \quad (k=1,2,3) \qquad (2.1)$$

where c,d_k,e_k are dimensionless numbers describing the instrument in terms of the calibration standards.

Equation (2.1) represents three circles in the complex Γ plane and Γ is calculated from their common intersection. If $c\neq 0$ then the coordinates (in the Γ plane) of the centres vary with Γ but the condition $c=0$ can be realised by isolating the reference detector from the wave reflected by the DUT. It is usual for design purposes to assume $c=0$ and sufficient to do so if calibration procedures not relying on this approximation are used. With this approximation, equation (2.1) can be written as:

$$R_k^2 = D_k^2(P_k/P_R) = |\Gamma - f_k|^2 \quad (k=1,2,3) \qquad (2.2)$$

where

$$D_k = |d_k|^{-1} \text{ and } f_k = -(e_k/d_k)$$

Equation (2.1) describes for each k a circle in the complex plane centred at f_k and of radius $R_k = D_k\sqrt{P_k/P_R}$ and the diagrammatic representation of Figure 2

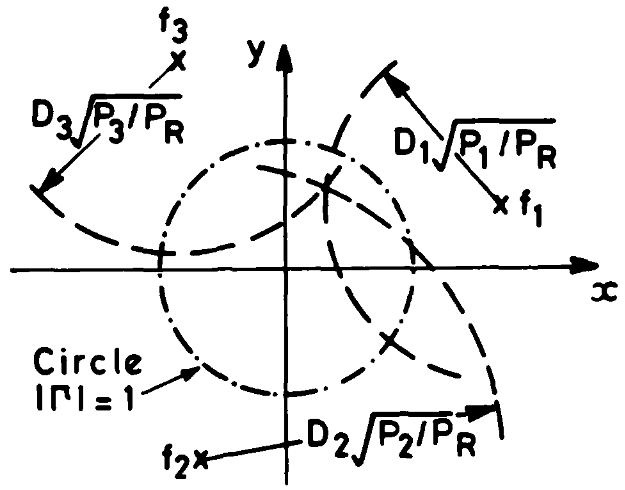

Figure 2 Circle diagram for reflectometer

assumes the necessary condition that the three f_k are different from each other so that the circles intersect uniquely in Γ. In Appendix A derivations of equations of the form of (2.2) are presented for four different designs of six-port junction (4,15,16,19,22).

Noise present in the output of each detector will cause uncertainty in determining each R_k and we can represent this by a rectangular probability distribution of R_k between limits of $\pm\Delta R_k$ caused by an equivalent noise power P_N for each detector. Then, from equation (2.1):

$$R_k \pm \Delta R_k = D_k \sqrt{(P_k \pm P_N)/(P_R \mp P_N)}$$

$$= D_k \sqrt{P_k/P_R}\,(1 \pm P_N/P_k)^{\frac{1}{2}}\,(1 \mp P_N/P_R)^{-\frac{1}{2}}$$

Assuming that $P_N << P_k$ and $P_N << P_R$ then

$$R_k \pm \Delta R_k \simeq R_k\left(1 \pm \frac{1}{2}(P_N/P_k + P_N/P_R)\right)$$

$$\frac{\Delta R_k}{R_k} \simeq \frac{1}{2}\left(\frac{1}{P_k} + \frac{1}{P_R}\right) P_N \qquad (2.3)$$

Equation (2.3) shows that the minimum fractional uncertainty in determining radius R_k would be when detector k and the reference detector both receive the maximum permitted detector power P_D(for $\frac{\Delta R_k}{R_k} = \frac{P_N}{P_D}$ when $P_k = P_R = P_D$). This minimum fractional uncertainty cannot be achieved for all Γ but, with c=0, the power absorbed by the reference detector is a constant sample of the power associated with the wave incident on the junction so that the resolution of measuring this sample would be maximised by operating with $P_R = P_D$. If the design is such that $P_R < P_D$ (because another detector absorbs P_D for some value of Γ with $P_R < P_D$) then the estimated uncertainty can be scaled by the multiplier P_D/P_R. Thus we can write, as a starting point, equation (2.3) as:

$$\frac{\Delta R_k}{R_k} = \frac{1}{2}\left(1 + \frac{P_D}{P_k}\right)\frac{P_N}{P_D} \tag{2.4}$$

Since P_D is the maximum power that can be absorbed by a detector and P_N is the equivalent noise power at a detector, P_D/P_N represents the maximum detector signal-to-noise ratio. Equation (2.4) enables ΔR_k to be calculated from this ratio for any Γ with the aid of the reflectometer design equation (2.2).

In the region of the intersection of the circles of radius R_1, R_2 and R_3 (from which Γ is calculated), each pair of limits (ΔR_1, ΔR_2), (ΔR_2, ΔR_3), (ΔR_3, ΔR_1) defines a curvilinear parallelogram within which Γ lies, as illustrated in Figure 3(a). Because $\pm R_k$ are the limits of a rectangular probability

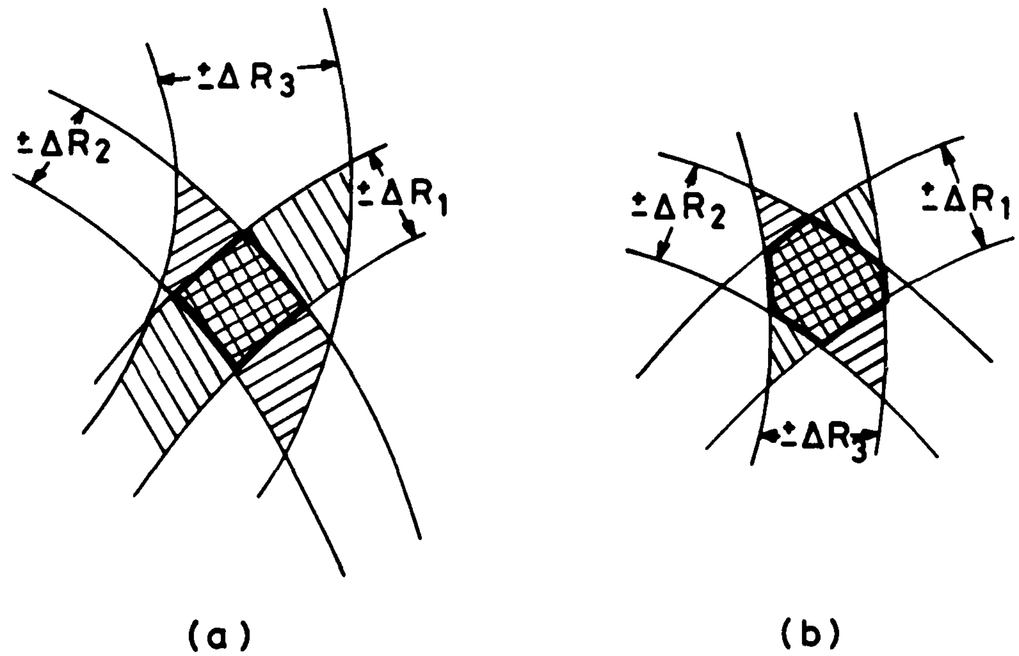

Figure 3 Areas of uncertainty of intersection

distribution of R_k, it is certain that Γ lies within the smallest of these three curvilinear parallelograms - as shown by the cross-hatched area of Figure 3(a). For those Γ for which all three ΔR_k are approximately equal, the area of uncertainty would be a curvilinear hexagon (as illustrated in Figure 3(b)) but, in that case, an estimate based on the smallest of the three parallelograms will be pessimistic and, therefore, safe. We now observe that for the parallelograms of interest, $\Delta R_k << \Delta R_k$. This follows, for when one of the R_k is small then, for a well designed junction, the remaining two are large and this is sufficient - as can be seen from Figure 2, for if Γ were to approach f_1, for example, then the intersection of R_2 and R_3 could be found with great precision and the only function of R_1 would be to resolve the ambiguity of which of the two intersections of R_2 and R_3 relates to Γ. With the assumption that $\Delta R_k \ll R_k$ we may approximate each area of uncertainty by a rectilinear parallelogram, as shown in Figure 4, which allows the cosine law to be used for calculating the maximum diagonal 2U from:

$$U = (\Delta R_1)^2 + (\Delta R_2)^2 + 2(\Delta R_1)(\Delta R_2)|\cos\theta|)^{\frac{1}{2}}/\sin\theta \qquad (2.5)$$

Equations (2.2), (2.4) and (2.5) allow the limits of $\pm U$ to be estimated for any Γ as the smallest of the three semi-diagonal lengths U obtained by treating the three ΔR_k in pairs.

2.2 Relating the limits of $\pm U$ so calculated to the measurement of Γ relies on the fact that the angular orientation of the maximum diagonal of Figure 4, relative to the x-y axes in the Γ plane, has no significance until the reflectometer has been calibrated with external standards. This means that the range

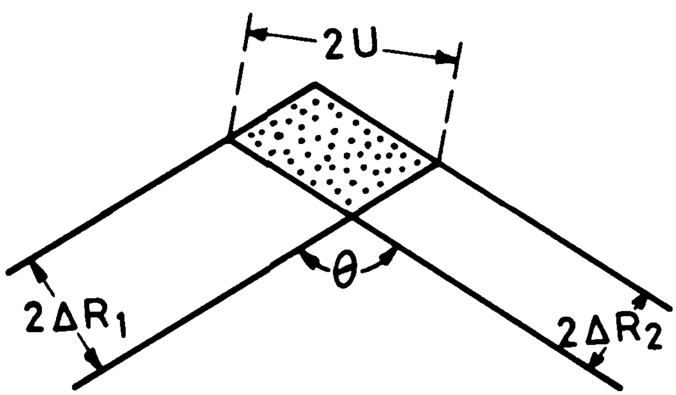

Figure 4 Rectilinear approximation

$-U$ to $+U$ can be regarded only as defining the diameter of a circle of confusion (to borrow a term from optics) within which it is certain that Γ lies (certain, that is, to the extent allowed by our approximations). Hence the estimated uncertainty in measuring magnitude $|\Gamma|$ is $\pm U$ and in measuring phase angle $\angle\Gamma$ is $\pm$ arctan $(U/|\Gamma|)$. Finally, we can compute each U for a net of different Γ covering the $|\Gamma| = 1$ radius circle and select the largest to provide an estimate of the maximum uncertainty U_{max} in measuring any $|\Gamma| \leq 1$. This procedure has been followed with a net of 321 different values of Γ, evenly spaced over the $|\Gamma| = 1$ radius circle, in estimating the values of U_{max} presented in section 4 for different designs of junction.

3 MAXIMUM POWER P_{max}

3.1 In section 2 we have postulated that the reference detector (i) is isolated from the wave reflected from the DUT and (ii) absorbs the maximum permitted detector power P_D. The net power supplied to the reflectometer and DUT from a matched source with available power output P_D will vary with Γ but a consequence of (i) is that P_R is a constant fraction F of P_o, irrespective of Γ, so that:

$$P_R = FP_o \qquad (3.1)$$

A consequence of (ii) is that it is necessary to check whether the condition $P_R = P_D$ to maximise resolution in measuring P_R can be met and, if not, to scale each computed U_{max} by P_D/P_R.

3.2 For each k, the maximum of P_k for all $|\Gamma|<1$ will be given, from equation (2.2), by:

$$\frac{P_{kmax}}{P_R} = \frac{(1 + |f_k|)^2}{D_k^2}$$

For one of the three k (say k=n), P_{nmax} will be the greatest of the three P_k, so that

$$\frac{P_{nmax}}{P_R} = \frac{(1 + |f_n|)^2}{D_n^2}$$

But $P_{nmax} \ngtr P_D$, so that the limiting condition is $P_{nmax} = P_D$, for which:

$$\frac{P_D}{P_R} = \frac{(1 + |f_n|)^2}{D_n^2} \tag{3.2}$$

Ideally then, we require that $(1 + |f_n|)^2/D_n^2 = 1$ and, if not, the computed U_{max} must be scaled by the value of P_D/P_R given by equation (3.2). Finally, the maximum power that can be incident on the junction to minimise U_{max} is, from equations (3.1) and (3.2):

$$P_o = \frac{D_n^2 P_D}{F(1 + |f_n|)^2} \tag{3.3}$$

In section 4 we present the results of applying the procedure using equations (3.1) to (3.3), and that derived in section 2, to compare the four designs of six-port junction detailed in Appendix A.

4 OPTIMISING U_{max}

4.1 Four of the cited designs of junction (4,15,16, 19 and 22) have been demonstrated to cover a frequency bandwidth at least equal to that of rectangular waveguide without the use of either switches or manual adjustment (after initial setting-up) and should therefore be stable. They each comprise between two and four conventional 90° hybrids (3 dB couplers) plus an input directional coupler, at which the source is connected. We show in this section that the coupling factor C of the input coupler (where $C = 20 \log_{10}(1/c)$, the voltage transmission and coupling coefficients being t and c, respectively, such that $|t|^2+|jc|^2 = 1$) can be chosen for each design to minimise U_{max}. In Appendix A we provide for completeness a derivation of equation (2.2) for each design and in Tables 1 to 4 we summarise the computed values of the following quantities of interest:-

(a) coupling factor CdB

(b) minimum ratio P_D/P_R when the power received by any detector $\ngtr P_D$.

(c) U_{max} (P_D/P_N) for P_R equal to its maximum permitted value.

(d) P_{max} in terms of P_D.

(e) the maximum power, in terms of P_D, absorbed by a matched DUT(W).

(f) the value of Γ giving $U_{max}(P_D/D_N)$

4.2 TABLE 1 - for design of reference (4)

CdB	P_D/P_R	$U_{max}\frac{P_D}{P_N}$	P_{max}/P_D	W/P_D	Γ for U_{max}
(a)	(b)	(c)	(d)	(e)	(f)
3	4.01	14.01	2.00	1.00	+1.0+0.0j
6	2.92	12.19	1.83	0.48	+1.0+0.0j
10	2.09	12.17*	2.12	0.21	-0.8+0.0j
20	1.30	20.05	3.10	0.03	-1.0+0.0j

4.3 TABLE 2 - for design of reference (15) for angle $2\alpha = 120^o$, giving largest U_{max} (see Appendix A)

CdB	P_D/P_R	$U_{max}\frac{P_D}{P_N}$	P_{max}/P_D	W/P_D	Γ for U_{max}
(a)	(b)	(c)	(d)	(e)	(f)
3.0	1.00	13.80	2.0	0.13	+0.4+0.1j
3.4	1.00	12.06*	2.2	0.14	+0.4+0.0j
6.0	2.48	21.53	4.0	0.19	-0.4-0.9j
10.0	7.48	53.79	10.0	0.23	-0.6-0.8j

4.4 TABLE 3 - for design of reference (16) which coincides with that of reference (15) at mean guide wavelength (when $2\alpha=90^o$)

CdB	P_D/P_R	$U_{max}\frac{P_D}{P_N}$	P_{max}/P_D	W/P_D	Γ for U_{max}
(a)	(b)	(c)	(d)	(e)	(f)
3.0	1.00	11.81	2.0	0.13	+0.2-0.1j
4.0	1.00	9.30*	2.5	0.15	+0.3-0.1j
6.0	1.95	13.15	4.0	0.19	+0.5-0.1j
10.0	5.89	32.50	10.0	0.23	+0.0-1.0j

4.5 TABLE 4 - for design of references (19,22)

CdB	P_D/P_R	$U_{max} \frac{P_D}{P_N}$	P_{max}/P_D	W/P_D	Γ for U_{max}
(a)	(b)	(c)	(d)	(e)	(f)
3.0	1.00	14.13	2.0	0.13	+0.5+0.0j
4.8	1.00	8.30*	3.0	0.17	+0.6+0.0j
6.0	1.49	9.92	4.0	0.19	+0.6+0.0j
10.0	4.50	18.69	10.0	0.23	+0.7-0.7j

4.6 The ratio P_D/P_N represents the maximum possible signal-to-noise ratio for any detector and, if this is known for a particular instrumentation system to be used with the junction, then the worst case uncertainty in measuring any $|\Gamma|\leq 1$ can be estimated from Tables 1 to 4. (For example, if the output of each detector is proportional to RF power absorbed and if all the proportionality factors are the same then, if the full range of a binary n-bit analogue-to-digital convertor represents P_D and $\pm$ (half the least significant bit) represents $\pm P_N$ then the estimated uncertainty in measuring any $|\Gamma|\leq 1$ is $U_{max}(P_D/P_N)/2^{n+1}$ worst case). In the absence of specific information on instrumentation, the tables still provide a comparison of the extent to which the different designs degrade the maximum P_D/P_N ratio, since the tabulated $U_{max}(P_D/P_N)$ represents this degradation even when the maximum permissible power is incident on the junction. The values that are starred (thus*) in Tables 1 to 4 represent the minimum $U_{max}(P_D/P_N)$ achieved for each design by selection of the input coupling factor C, *showing that the procedures* derived in section 3 enable the resolution of each design to be optimised.

5 PRACTICAL CONSIDERATIONS

5.1 Tables 1 to 4 provide data for comparing different designs of junction each with different values of input coupling but there is lacking a single criterion for such a comparison. In practice, there is need to compromise between the conflicting requirements to:

(a) minimise the measurement uncertainty (and Table 4 shows that the design of references 19, 22 achieves this)

(b) minimise the RF source power P_o in order to minimise the cost, particularly for use at millimetric wavelengths (and Table 1 shows that the design of reference 4 achieves this)

(c) minimise the power incident on a matched load, to minimise over-loading semiconductor devices under test (see the column W/P_D in Tables 1 to 4)

(d) simplify experimental evaluation by using off-the-shelf directional couplers

(e) allow planar construction to permit possible development to other transmission media, including E-plane split waveguide, microstrip, image guide or dielectric guide (of the designs shown in Appendix A, only those of references 15 and 16 are easily adaptable to all these media)

(f) use the minimum of components to (hopefully) minimise the departure of practical performance from that predicted by simple theory (design of reference 15)

(g) not assume equality of phase velocity in the directional couplers to that in the interconnecting leads (and the analyses of Appendix A show that this applies to references 4 and 16 only).

5.2 Experience at RSRE in different frequency bands ranging from 10 MHz to 100 GHz with single reflectometers of each of the designs considered shows that, with the instrumentation used, the uncertainty of measurement of Γ is limited by the repeatability of connection of precision coaxial connectors and waveguide flanges. At first sight, therefore, this reported work aimed at minimising the contribution of junction design to this uncertainty seems superfluous. However, the utility of dual six-port network analysers (D6 PNA) will depend in part on their range of attenuation measurement and this depends on the uncertainty $\Delta|\Gamma|$. It can be shown from equation (4.2) of ref (23) that the span S of attenuation produced by a matched attenuator that could be measured with a D6PNA to a precision of ±1 dB is

$$S = 20 \log_{10}(2^{n+1}(10^{0.05} - 1)/\Delta|\Gamma|) \text{ dB}$$

when an n-bit A to D convertor is used (see para 4.6). We have tabulated in Table 5 values of S that would be obtained with n = 16 when P_o is (i) equal to P_{max} and (ii) equal to 1.83 P_D. Condition (i) gives the maximum obtainable S for each design and condition (ii) allows comparison of S when all the junctions considered are subject to the minimum power tabulated in column 4 of Tables 1 to 4. The values of S tabulated are slightly pessimistic, for they have been calculated using the worst case $\Delta|\Gamma|$ throughout. The coupling factors tabulated correspond to the coupling coefficients C_1 to C_4 of Appendix A and they have been restricted to values obtainable for off-the-shelf directional couplers.

Table 5

		Design Reference									
		(4)			(16)			(19,22)		(15)	
Coupling factor dB	C_1	3	6	10	3	3	6	3	6	3	6
	C_2	3	3	3	3	3	3	3	3	3	3
	C_3	3	3	3	3	6	3	3	3	3	3
	C_4	3	3	3	3	3	3	3	3	-	-
	C_5	3	3	3	-	-	-	-	-	-	-
P_{max}/P_D		2.00	1.83	2.12	2.0	2.0	4.0	2.0	4.0	2.0	4.0
$S(P_{MAX})$	dB	61.2	62.4	62.4	63.1	63.9	61.7	61.1	64.2	61.3	57.4
$S(1.83P_D)$	dB	60.4	62.4	61.1	62.3	63.1	54.9	60.3	57.4	60.5	50.6
					(2)	(1)					

Table 5 shows that the design represented by the column marked (1) has the greatest $S_{(1.83P_D)}$ value and that its $S_{(P_{max})}$ value is only 0.3 dB less than the maximum of these but it is achieved with 3 dB less power than that maximum. These factors, together with the desirable practical features listed in para 5.1, show that the designs represented by columns (1) and (2) are the first and second choices, respectively, for future practical work.

6 CONCLUSION

We have derived a numerical procedure for comparing different theoretical designs of six-port junction and have considered the desirable practical features of design. From this work we have established an "optimum" design for use in development of dual six-port network analysers and have, in doing so, established a practical benchmark for judging other published theoretical designs. We conclude that if the span of measurement of S_{21} with a D6PNA is to be increased much beyond 60 dB, then work on improving the detector signal-to-noise ratio is likely to be more worthwile than further work on six-port junction design.

NOTE: The design of reference (16) is now covered by UK Patent Application 8413339, May 1984.

7 REFERENCES

1 C A Hoer, "The six-port coupler: a new approach to measuring voltage, current, power, impedance, and phase", IEEE Trans, IM-21, 466-470, Nov 1972.

2 G F Engen and C A Hoer, "Application of an arbitrary six-port junction to power measurement problems", ibid, 470-474, Nov 1972.

3 G F Engen, "The six-port reflectometer: an alternative network analyser", IEEE Trans, MTT-25, 1075-1080, Dec. 1977.

4 G F Engen, "An improved circuit for implementing the six-port technique of microwave measurements", ibid, 1080-1083, Dec 1977.

5 R J Collier and N A El-Deeb, "Multistrip coupler suitable for use as a 6-port reflectometer", IEE Proc, 127, pt H, 87-91, Apr 1980.

6 A L Cullen, S K Judah and F Nikravesh, "Impedance measurement using a 6-port directional coupler", ibid, 92-98, Apr 1980.

7 H P Groll and W Kohl, "Six-port consisting of two directional couplers and two voltage probes for impedance measurement in the millimetre wave range", Proc 10th European Microw Conf, 295-298, Sep. 1980.

8 G P Riblet, "A compact waveguide "resolver" for the accurate measurement of complex reflection and transmission coefficients using the 6-port measurement concept",IEEE Trans, MTT-29, 155-162, Feb 1981.

9 D A Granville-George and D Woods, "Computer-controlled 6- port reflectometer for the frequency range 10 MHz to 1 GHz", IEE Colloq Digest 1981/49, 8/1-8/4, May 1981.

10 M Yeo, "A microwave integrated circuit six-port reflectometer", ibid, 12/1-12/9, May 1981.

11 J A Paul and P C H Yen, "Millimeter-wave passive components and six-port network analyser in dielectric waveguide", IEEE Trans, MTT-29, 948-953, Sep 1981.

12 E R Bertil Hanson and G P Riblet, "The matched symmetrical five-port junction as the essential part of an ideal six-port network", Proc 11th European Microw Conf, 501-506, Sept 1981.

13 U R Stumper, "A simple multiport reflectometer using fixed probes and an adjustable attenuator," ibid, 622-626.

14 D Radovich and J Paul, "Phase and amplitude characteristics of dielectric waveguide coupler and six-port network", IEEE MTT-S Digest, 322-324, May 1982.

15 E J Griffin, "Six-port reflectometer circuit comprising three directional couplers", Electron Lett, 18, 491-493, Jun 1982.

16 R J Collier and G Hjipieris, "An image guide six-port reflectometer", private communication, Mar 1983.

17 J A Dabrowolski, "Improved six-port circuit for complex reflection coefficient measurements", Electron Lett, 18, 748-750, Aug 1982.

18 E R Bertil Hansson and G P Riblet, "An ideal six-port consisting of a matched reciprocal lossless five-port and a perfect directional coupler", IEEE Trans, MTT-31, 284-288, Mar 1983.

19 UK Patent Application 8311170, May 1983.

20 B A Herscher and J E Carroll, "A 7-port reflectometer system implemented with a single combline directional coupler", IEE Colloq Digest, 1983/53, 10/1-10/7, May 1983.

21 C M Potter and C M Snowden, "Low cost integrated RF six-port", Electron Lett, 19, 815-816, Sep 1983.

22 E J Griffin, G J Slack and L D Hill, "Broadband six-port reflectometer junction", ibid, 921-922, Oct 1983.

23 T E Hodgetts and E J Griffin, "A unified treatment of the theory of six-port reflectometer calibration using the minimum of standards", RSRE Report No 83003, Aug 1983.

APPENDIX A

A.1 In this appendix we present, for completeness, a derivation of equation (2.2) for each of the designs considered. Throughout, complex numbers c_n and t_n are used to denote the voltage coupling and transmission coefficients, respectively, of the nth directional coupler and we assume the reference planes of each coupler to be positioned such that $|t_n|^2 + |jc_n|^2 = 1$. We refer to angles θ_n, α, and β, to denote the angular electrical lengths of various interconnecting waveguides and denote the voltages associated with waves incident on and emergent from the mth port of the complete junction by a_m and b_m, respectively. All components are assumed to be matched and lossless, so that the directional couplers have infinite directivity.

A.2 A diagram of the design of reference (4), drawn for Lange microstrip directional couplers (10) is given in Figure A.1.

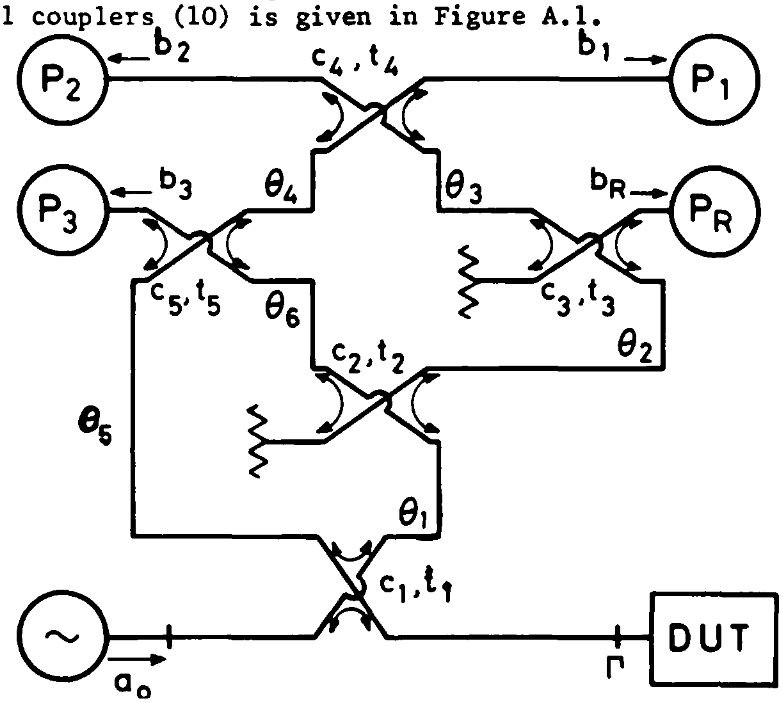

A1

Elementary circuit analysis shows that:

$$\frac{b_R}{a_o} = -t_1c_2c_3e^{-j(\theta_1+\theta_2)}$$

$$\frac{b_1}{a_o} = jc_1t_1t_4t_5e^{-j(\theta_4+\theta_5)}\left(\Gamma + \frac{t_2c_5}{c_1t_5}e^{-j(\theta_1+\theta_6-\theta_5)} + j\frac{c_2t_3c_4}{c_1t_4t_5}e^{-j(\theta_1+\theta_2+\theta_3-\theta_4-\theta_5)}\right)$$

$$\frac{b_2}{a_o} = -c_1t_1c_4t_5e^{-j(\theta_4+\theta_5)}\left(\Gamma + \frac{t_2c_5}{c_1t_5}e^{-j(\theta_1+\theta_6-\theta_5)} - j\frac{c_2t_3t_4}{c_1c_4t_5}e^{-j(\theta_1+\theta_2+\theta_3-\theta_4-\theta_5)}\right)$$

$$\frac{b_3}{a_o} = -c_1t_1c_5e^{-j\theta_5}\left(\Gamma - \frac{t_2t_5}{c_1c_5}e^{-j(\theta_1+\theta_6-\theta_5)}\right)$$

By arranging that $\theta_1+\theta_2=\theta_5$; $\theta_2=\theta_6$; $\theta_3=\theta_4$ and choosing $|c_2|=|c_3|=|c_4|=|c_5|=\frac{1}{\sqrt{2}}$ (ie 3 dB couplers) and writing c,t for $|c_1|,|t_1|$ then, since $P_R = |b_R|^2$ and $P_k = |b_k|^2$, where k = 1,2,3, the foregoing equations give the following coefficients for equation (2.2):

k	$D_k^{\ 2}$	f_k
1	$\frac{1}{c^2}$	$-\frac{1}{\sqrt{2}c}(1+j)$
2	$\frac{1}{c^2}$	$\frac{-1}{\sqrt{2}c}(1-j)$
3	$\frac{1}{2c^2}$	$\frac{1}{\sqrt{2}c} + j0$

A.3 In Figure A2, relating to the design of reference (15), we first denote

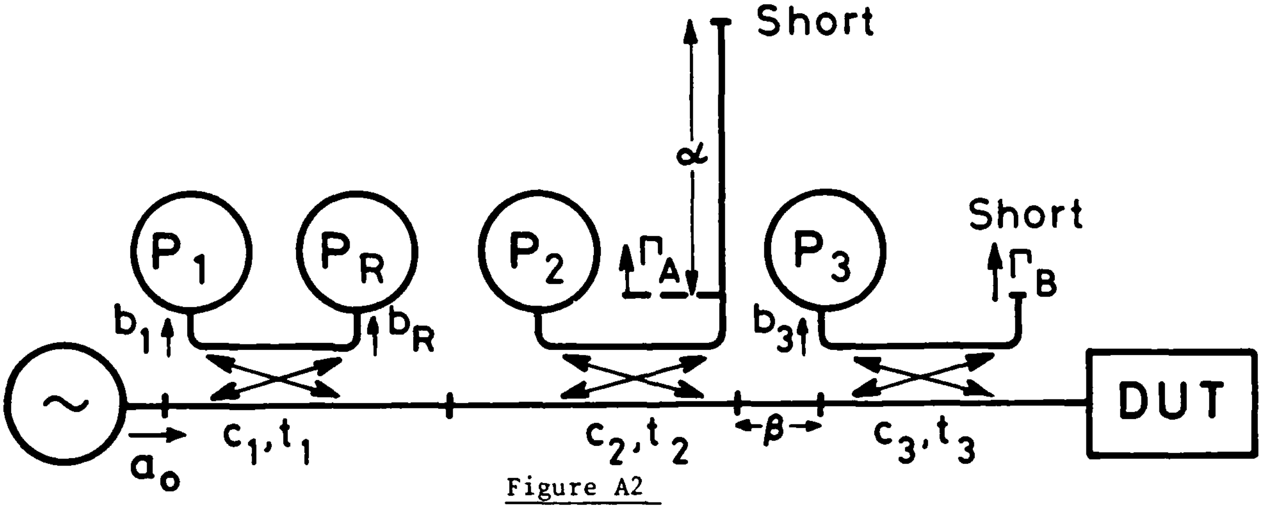

Figure A2

the voltage reflection coefficients (VRC) presented by the short circuits to couplers 2 and 3 by Γ_A and Γ_B, respectively. Then:

$$\left.\begin{aligned}
\frac{b_R}{a_o} &= jc_1 \\
\frac{b_1}{a_o} &= jc_1 t_1 t_2^2 t_3^2 e^{-j2\beta}\left(\Gamma - \frac{c_3^2}{t_3^2}\Gamma_B - \frac{c_2^2\Gamma_A}{t_2^2 t_3^2} e^{j2\beta}\right) \\
\frac{b_2}{a_o} &= jc_2 t_1 t_2 t_3^2 e^{-j2\beta}\left(\Gamma - \frac{c_3^2}{t_3^2}\Gamma_B + \frac{\Gamma_A}{t_3^2} e^{j2\beta}\right) \\
\frac{b_3}{a_o} &= jc_3 t_1 t_2 t_3 e^{-j\beta}(\Gamma + \Gamma_B)
\end{aligned}\right\} \qquad \text{(A.1)}$$

But $\Gamma_A = -e^{-j2\alpha}$ and $\Gamma_B = -1$, so that choosing $\beta = 0$ and $|c_1| = |c_2| = |c_3| = 1/\sqrt{2}$ and $\alpha = (\theta_3 + \pi/4)$ at the mean guide wavelength (where $t_3 = |t_3|e^{-j\theta_3}$), give the following coefficients in equation (2.2):-

k	D_k^2	f_k
1	$16/t^2$	$-1-2(\cos 2\alpha - j\sin 2\alpha)$
2	$16c^2/t^2$	$-1+2(\cos 2\alpha - j\sin 2\alpha)$
3	$8c^2/t^2$	$1 + j0$

We note that as the frequency is increased over the bandwidth of rectangular waveguide, 2α increases from 60° to 120° and U_{max} increases also; for this reason, Table 2 has been calculated for $2\alpha = 120^\circ$.

A.4 A modification of the design of reference (15) produces the broadband design (16) illustrated in Figure A3. Equations (A.1) apply to this

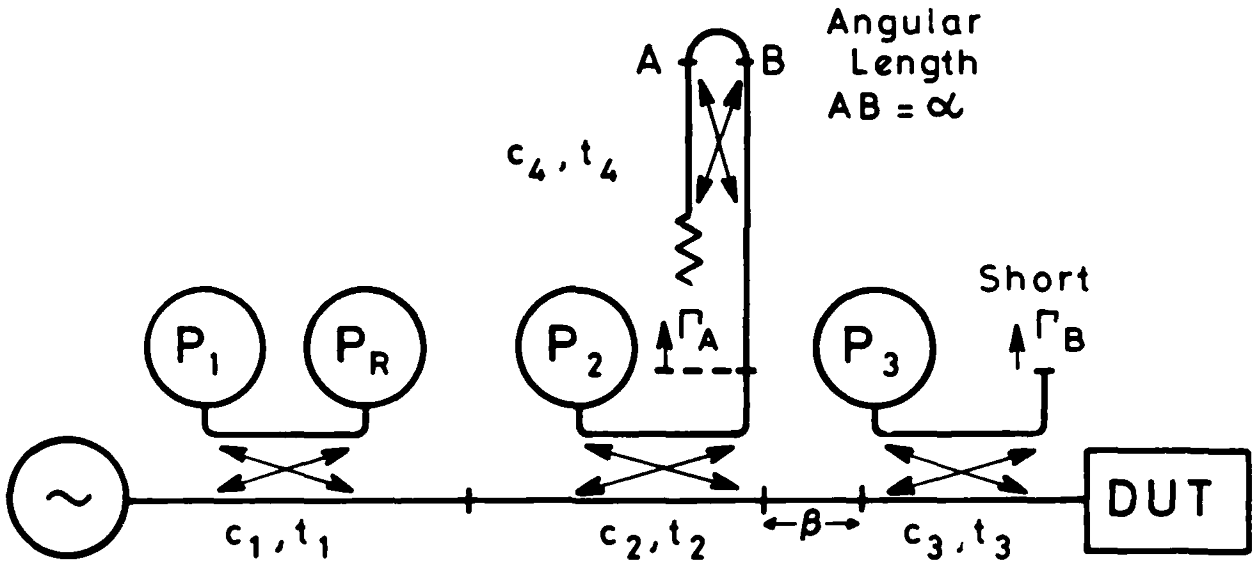

A3

junction also, but Γ_A has to be evaluated for them to be applied. Using, for the moment, a_m, b_m to refer to coupler 4, as shown in Figure A4 (so that $\Gamma_A = b_1/a_1$) then, by inspection:

$b_1 = ta_2 + jca_4$

$b_2 = ta_1 \quad (\because a_3 = 0)$

$b_3 = jca_2 + ta_4$

$b_4 = jca_1 \quad (\because a_3 = 0)$

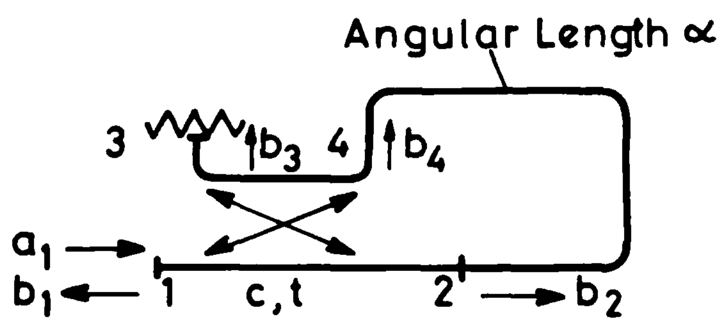

Figure A4

With length of waveguide α connecting ports 2 and 4,

$$a_2 = b_4 e^{-j\alpha} \text{ and } a_4 = b_2 e^{-j\alpha}$$

Whence $\dfrac{b_3}{a_1} = (t^2 - c^2)e^{-j\alpha}$ and $\dfrac{b_1}{a_1} = 2jct\ e^{-j\alpha} = \Gamma_A$

For the complete junction, with $\Gamma_B = -1$, $\Gamma_A = 2jc_4t_4e^{-j\alpha}$ and $\beta = \alpha/2$ in equations (A.1), the coefficients of equation (2.2) become:-

k	D_k^2	f_k
1	$16/t^2$	$-1 + j2$
2	$16c^2/t^2$	$-1 - j2$
3	$8c^2/t^2$	$1 + j0$

A.5 The diagram describing the design of references (19, 22) is shown in

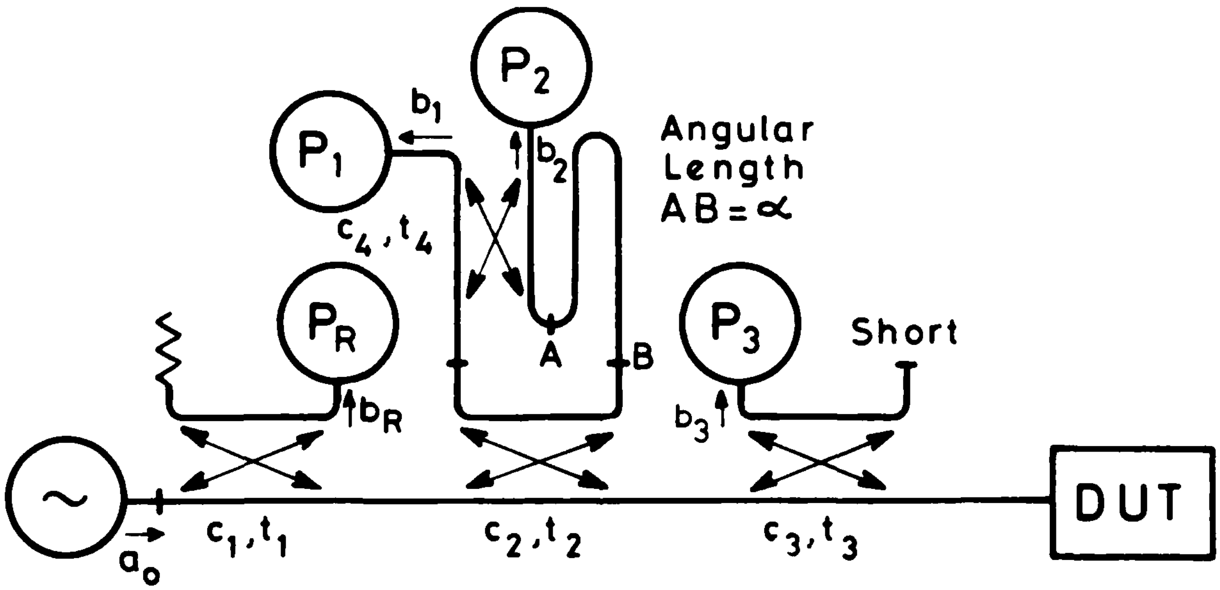

Figure A5

Figure A.5 from which, by inspection:-

$$\frac{b_R}{a_o} = jc_1$$

$$\frac{b_1}{a_o} = jt_1c_2t_2t_3^2t_4\left(\Gamma + \frac{c_3^2}{t_3^2} + j\,\frac{c_4e^{-j\alpha}}{t_2t_3^2t_4}\right)$$

$$\frac{b_2}{a_o} = -t_1c_2t_2t_3^2c_4\left(\Gamma + \frac{c_3^2}{t_3^2} - j\,\frac{t_4e^{-j\alpha}}{c_4t_2t_3^2}\right)$$

$$\frac{b_3}{a_o} = jt_1t_2c_3t_3(\Gamma - 1)$$

With $|c_3|=|c_4|= 1/\sqrt{2}$ and $\alpha = \theta_2 + 2\theta_3$ (where $t_2 = e^{-j\theta_2}/\sqrt{2}$ and $t_3 = e^{-j\theta_3}/\sqrt{2}$), these equations lead to the following coefficients in equation (2.2):-

k	D_k^2	f_k
1	$32c^2/t^2$	$-1 - j2\sqrt{2}$
2	$32c^2/t^2$	$-1 + j2\sqrt{2}$
3	$8c^2/t^2$	$1 + j0$

DOCUMENT CONTROL SHEET

Overall security classification of sheet UNCLASSIFIED

(As far as possible this sheet should contain only unclassified information. If it is necessary to enter classified information, the box concerned must be marked to indicate the classification eg (R) (C) or (S))

1. DRIC Reference (if known)	2. Originator's Reference Memorandum 3684	3. Agency Reference	4. Report Security Classification Unclassified
5. Originator's Code (if known)	6. Originator (Corporate Author) Name and Location Royal Signals and Radar Establishment		
5a. Sponsoring Agency's Code (if known)	6a. Sponsoring Agency (Contract Authority) Name and Location		

7. Title
COMPARING DIFFERENT THEORETICAL DESIGNS OF SIX-PORT REFLECTOMETER JUNCTIONS

7a. Title in Foreign Language (in the case of translations)

7b. Presented at (for conference papers) Title, place and date of conference

8. Author 1 Surname, initials	9(a) Author 2	9(b) Authors 3,4...	10. Date	pp. ref.
Griffin E J	Hodgetts T E			

11. Contract Number	12. Period	13. Project	14. Other Reference

15. Distribution statement
Unlimited

Descriptors (or keywords)

continue on separate piece of paper

Abstract

This memorandum presents a derivation of numerical procedures for comparing different theoretical designs of six-port junctions for use in measuring the voltage reflection coefficient Γ of passive loads ($|\Gamma| \leqslant 1$). It shows from these that the maximum uncertainty in measuring any passive load can be minimised by a suitable choice of components, in each of four different designs, and discusses the relative merits of these designs in terms of selecting a best compromise for use in a dual six-port network analyser.

END

FILMED

2-85

DTIC